Combined methodologies for gaining much information from ancient dental calculus: testing experimental strategies for simultaneously

(Article begins on next page)

20 December 2021

Combined methodologies for gaining much information from ancient dental calculus: testing experimental strategies for simultaneously analysing DNA and food residues.

Alessandra Modi[1], Lisa Pisaneschi[2], Valentina Zaro[1], Stefania Vai[1], Chiara Vergata[1], Enrico Casalone[3], David Caramelli[1], Jacopo Moggi Cecchi[1], Marta Mariotti Lippi[2†], Martina Lari[1†]

1 Department of Biology, University of Florence, Via del Proconsolo 12, Florence, Italy

2 Department of Biology, University of Florence, Via La Pira 4, Florence, Italy

3 Department of Biology, University of Florence, Via Madonna del Piano 6, Sesto Fiorentino, Italy

† These authors contributed equally to this work

Correspondence and requests should be addressed to:

Martina Lari: martina.lari@unifi.it

Alessandra Modi: alessandra.modi@unifi.it

Abstract

Dental calculus from archaeological samples is a rich source of ancient biomolecules, such as DNA, proteins, and microremains, mainly related to food. Focusing on different contents, laboratory procedures require specific treatments that necessitate the same material and are generally mutually exclusive; therefore, the low quantity of the starting material is often the main limiting factor for gathering data.

Here, we compare different combinations of laboratory procedures in order to identify the best strategy for simultaneously extracting DNA and isolating plant residue. Preliminary tests were performed on fresh plant materials to verify the effects of the DNA extraction protocols on starch grains and phytoliths. Different combined experimental procedures were successively applied to the dental calculus of three medieval individuals.

Our results confirmed that authentic genetic data could be recovered from ancient dental calculus using protocols commonly used for extracting DNA from ancient bones and teeth, and the residual pellet could be

1

successfully used for morphological characterization of plant residues. In addition, we confirmed that, although most DNA within calculus is microbial, the whole human mitochondrial genome could be reconstructed using target enrichment techniques.

Keywords: starch grains, phytoliths, microbiome, mitochondrial DNA, Medieval burial

Introduction

Over the past two decades, dental calculus has become the subject of an increasing number of investigations that concern different research fields in biology. This growing interest is due to its chemical nature and way of forming (Warinner et al. 2015), which make tartar a mineralized archive of multisource residues deriving from the oral cavity, including mucosa cells, components of the bacterial flora, and minute fragments of various materials that entered the mouth. Indeed, acting as a trap for numerous debris fragments, dental calculus can provide information about human health, hygiene, behaviours and activities that characterize recent or ancient cultural contexts (Radini et al. 2016); the kind of the information depends on the origin of the residue. An exhaustive list of the possible sources of debris and the information that may be acquired was recently provided by Radini et al. (2017).

Recent dental calculus analyses mainly deal with the oral microbiome (e.g., Adler et al. 2013; Mann et al. 2018; Warinner et al. 2014a, 2015; Weyrich et al. 2015, 2017), the stable isotope ratio (e.g., Cristiani et al. 2018; Huynh et al. 2016; O'Regan et al. 2016; Scott and Poulson 2012; Wang et al. 2015), and X-ray spectrometry and mass spectrometry of trace elements (Lazzati et al. 2016), in order to collect data about the consumption of animal and plant food; the food residues are mainly represented by starch grains and phytoliths (e.g., Hart 2011, 2016; Henry et al. 2014).

Laboratory procedures focusing on different contents require specific treatments that have been developed independently and are usually applied separately. As a consequence, the amount of tartar recovered from the teeth has become the main limiting factor for gathering data; hence, there is a requirement to develop combined protocols for gaining considerable amount of information from the same archaeological sample source (Rusu et al. 2018).

At present, the sample quantity to be analysed in each study and the strategies that could be the most advantageous in sampling and processing dental calculus are not established (Warinner et al. 2015), and the choice of strategy mainly depends on the availability of the material on a case by case basis. Additionally, the teeth of individuals from archaeological excavations are often cleaned along with other findings recovered at the sites. In these situations, the hope of gathering new information leads to carrying out dental calculus analyses on the scarce quantities recovered from the teeth of individuals from famous

2

archaeological sites, and the type of investigation that is considered the most promising in each context is chosen. However, the method of choice may not be the most advantageous.

This situation has led us to attempt to combine laboratory procedures to study the microbiome and the plant residues in the same sample of dental calculus instead of dividing it in two subsamples. Preliminary tests were performed on modern fresh material to verify the consequences of the DNA extraction protocols on the preservation of starch grains and phytoliths. Two different combined procedures were successively used to study the dental calculus of individuals recovered from the medieval cemetery adjacent to the church of Sant'Angelo in Pescheria in the centre of Rome, dated between the 9th and 13th century CE, in the area formerly known as *Porticus Octaviae* (Ciancio Rossetto 2008) (see Electronic Supplementary Material).

Dental calculus studies from Italian archaeological sites are not numerous. The different methodologies of these studies have mainly been aimed at understanding the dietary habits of ancient populations. Analyses of plant remains in the calculus of individuals of a Copper-Bronze Age population at Scoglietto in Central Italy (Mariotti Lippi et al. 2017) provided evidence for the consumption of a variety of crops, including millets; these data were crossed with the results of the stable isotope ratio in the bone collagen recorded in the same population (Varalli et al. 2015). Mass spectrometry in Bronze Age populations at numerous sites, including Olmo di Nogara in Northern Italy and Isola Sacra in Central Italy (Warinner et al. 2014b), provided evidence for the consumption of milk; the same approach was used for samples from Bovolone in Northern Italy and from Sant'Abbondio in Southern Italy, also revealing milk consumption in the Middle Bronze Age (Soncin et al. 2016). Morphological analyses of the debris fragments in dental calculus was performed at the Etruscan-Celtic necropolis of Monterenzio Vecchia, Northern Italy (Charlier et al. 2010), in order to evaluate the potentiality of this type of analysis in forensic anthropology. Finally, X-ray spectrometry, mass spectrometry of trace elements, and plant residue analysis were performed on dental calculus of medieval individuals from Caravate, Northern Italy (Lazzati et al. 2016). The analysis suggested a diet based on the consumption of carbohydrates, mainly derived from Poaceae, and proteins, mostly from fish.

Materials and Methods

1. Preliminary tests on fresh plant materials.

Two different decontamination methods ("a", "b") and three decalcification and digestion methods ("c", "d", "e") were tested on different samples of starch grains and phytoliths. The aim of the tests was to verify the possible onset of damages on these plant materials during the treatments commonly used to extract DNA from ancient dental calculus. Briefly, in method "a", starch grains and phytoliths were briefly incubated with 1% sodium hypochlorite, while in method "b", a 0.5 M solution of EDTA was used; in methods "c", "d", "e", different combinations of decalcification and protein digestion agents were tested under various conditions of incubation time and temperature (see Electronic Supplementary Material for details). Both

decontamination ("a", "b") and decalcification/digestion ("c", "d", "e") methods were selected according to previous molecular studies on dental calculus (Adler et al. 2013; Warinner et al. 2014a).

Starch grains were obtained from the flour of *Triticum aestivum L.* and *Cicer arietinum L.* Phytoliths were isolated from *Bambusa sp*. leaves collected in the Botanical Garden of the University of Florence. To simulate different states of preservation of the phytoliths, *Bambusa* leaves were treated according to two different methodologies (Piperno 2006, Electronic Supplementary Material): 1 - Dry ashing method, which involved ignition at 500°C for two hours; 2 - Wet oxidation method, which involved chemical treatment with 65% nitric acid for 30 minutes.

Fresh starch grains and phytoliths were divided into several subsamples to test the effects of decontamination and decalcification/digestion methods both individually (a, b, c, d, e) and in combinations (a+c, a+d, a+e, b+c, b+d, b+e). In total, 11 different assays were set up for each sample (Fig. S1 and Electronic Supplementary Material). Morphometric features of the treated material were examined under a light microscope (l.m.) and polarizing l.m., and the results were compared with the observations from the reference untreated material. The possible loss of starch grains as a consequence of the methods was estimated as the variation of the grain size distribution with respect to the untreated material, calculated in a known volume. This analysis allowed us to test if the loss mainly affects the dimensional range of the grains.

2. Comparison of different procedures for the analysis of ancient dental calculus.

To identify the best strategy for simultaneously extracting DNA and identifying plant microremains from ancient dental calculus, different experimental procedures were compared. Dental calculus was sampled from three individuals (P.O 108-7, P.OZ. US44, and P.O 898-11) buried in the medieval cemetery of the church of Sant'Angelo in Pescheria (Rome) (see Electronic Supplementary Material), each of which displayed abundant deposits of dental calculus (Fig. 1, Table 1 and Electronic Supplementary Material). For each individual, the calculus retrieved from different teeth (Fig. 1, Electronic Supplementary Material) was combined into a single tube, coarsely ground with a sterile micropestel, and then divided into three sub-samples of approximately the same weight (Table 1). The three sub-samples were processed as described below:

Procedure A: Dental calculus was washed with 1 mL of 0.5 M EDTA to remove the environmental contaminants. The sample was then crushed in a 2 mL tube with a sterile micropestel in order to obtain a coarse powder that was subsequently incubated in 1 mL of extraction buffer (0.45 M EDTA, 0.25 mg/mL Proteinase, 0.05% Tween 20) overnight at 37°C. The pellet resulting from the digestion step was used for plant microremains extraction (Henry and Piperno 2008; see Procedure B), while DNA was extracted from supernatant using a silica-based protocol (see below).

Procedure B: After a short rinsing in boiling water, dental calculus was processed as described in Henry and Piperno (2008): dental calculus was incubated in a 10% solution of sodium hexametaphosphate for 24 h. The

4

sample was then ultra-sonicated for 5 minutes and incubated in 10% HCl for 12 h. The presence of starch grains and phytoliths was investigated using l.m.

Procedure C: Dental calculus was treated as described in Procedure B. After sonication, dental calculus was washed twice with H_2O and then incubated in the same extraction buffer and incubation conditions used in Procedure A. After centrifugation, the supernatant was used for DNA extraction (see below), while the pellet was incubated in 10% HCl for 12 h and then investigated by optical microscopy for the analysis of plant microremains.

A summary of the experimental design is reported in Fig. 2. Additional details of each procedure are described in Electronic Supplementary Material.

3. Analysis of plant microremains in ancient dental calculus.

Analysis of plant microremains was performed at the Laboratory of Plant Biology, University of Florence. As previously described, the pellets resulting from Procedure A and Procedure C, as well as the material treated with sodium hexametaphosphate in Procedure B, were incubated with a 10% HCl solution for 12 h, then washed in distilled water and stored in a 50% (v/v) water-glycerol solution. Observations of starch grains and phytoliths were carried out under l.m. and polarizing l.m., operating at 400 magnification. Identification was performed on the basis of the morphometric features using literature (Henry et al. 2009; Piperno 2006; Seidemann 1966) and reference materials. Each starch grain or group was counted as one presence. Considering that Procedure B represents the protocol commonly used for recovering plant microremains from ancient dental calculus (Henry and Piperno 2008), the observations from the material processed with this approach were used as the reference control in the subsequent data comparisons. See Electronic Supplementary Material for more details.

4. Genetic analysis.

DNA was extracted in the clean-room facilities of the Laboratory of Molecular Anthropology and Paleogenetics, University of Florence, using a silica-based protocol specifically designed to improve the recovery of short degraded molecules (Dabney et al. 2013). Preventive measures were taken to avoid contamination during all the experimental procedures (Gilbert et al. 2005; Willerslev and Cooper, 2005). After DNA extraction from the digested supernatant obtained in Procedures A and C, DNA was quantified using Agilent 2100 Bioanalyzer (High Sensitivity DNA chip) and Qubit™ 4 Fluorometer (dsDNA High Sensitivity Kit).. Twenty microlitres of the extracts obtained from the dental calculus processed with Procedure A were then converted in double-stranded and double-indexed libraries according to Meyer and Kircher (2010) and Kircher et al. (2012). No uracil DNA glycosylase (UDG) treatment was performed to retain misincorporation patterns due to cytosine deamination in ancient DNA (Briggs et al. 2007). The fill-in reaction was split in 4 aliquots that were amplified separately in 100µl reaction mixes as described in Modi et al. (2017). Ten cycles of indexing PCR were performed by default on each library. The DNA

concentration of the libraries was measured with an Agilent 2100 Bioanalyzer (DNA 1000 chip), afterwards libraries were pooled in equimolar amounts and sequenced on Illumina MiSeq with 2x76+8+8 cycles. The EAGER pipeline (Peltzer et al. 2016) was used for initial quality control, adapter trimming, merging paired-end reads and mapping to the human reference genome. Non-human reads were then screened for oral microbiome composition using MetaPhlAn2 (Truong et al. 2015). A detailed description can be found in Electronic Supplementary Material. To verify that the oral microbiome signature is ancient rather than derived from modern contaminants, damage patterns were detected using mapDamage2.0 (Jonsson et al. 2013). MapDamage was performed for the reads mapping to the reference genomes of more abundant species typical of the human oral microbiome (see below and Electronic Supplementary Material for more details). In addition to profiling the degradation patterns, a source modeling approach was applied for authenticating microbiome samples (Warinner et al., 2017). SourceTracker (Knights et al., 2011) was used to estimate the microbiome preservation and evaluate the different contributing metagenome sources (see below and Electronic Supplementary Material for more details).

To obtain the human mitochondrial sequences of the individuals from the same dental calculus used for the plant microremains and oral microbiome composition analyses, the libraries was enriched for mtDNA using the in solution capture technique (Maricic et al. 2010) with specific modifications according to Ozga et al. (2016). Before capture, 10 µl of each library were amplified in ten parallel reactions (1 µl of template per reaction) using AccuPrime Pfx (Life Technology), as described in Ozga et al. (2016). After target enrichment, libraries were amplified and quantified using Agilent 2100 Bioanalyzer (DNA 1000 chip), pooled in equimolar amounts and sequenced on Illumina MiSeq with 2x75+8+8 cycles. After demultiplexing, raw reads were analysed using a specific pipeline optimized for ancient DNA (see Electronic Supplementary Material for more details). MtDNA haplogroup assignment was performed with Mitomaster (Brandon et al. 2009), which makes use of HaploGrep (Kloss-Brandstatter et al. 2011) based on PhyloTree Build 16 (van Oven and Kayser 2009).

The two mitochondrial sequences reported in this paper were submitted to NCBI GenBank under the accession numbers MK463535 and MK463536

Results and discussion

1. Preliminary tests on fresh plant materials.

The preliminary survey performed on untreated fresh flour and treated phytoliths allowed us to record the original morpho-metrical features of the reference material.

Starch grains - The *Triticum* flour consisted of two different dimensional classes of simple grains:

- Large grains had a lenticular tridimensional shape; by l.m., they appeared circular to ovoid in plane view and lenticular in side view. In plane view, the large grains measured (10) 15-30 (32.5) µm in diameter/main

6

axis and presented inconspicuous lamellae; under polarizing l.m., they sometimes displayed a symmetrical cross, with arms that widen at the ends. The large grain-size distribution was reported in Fig. S2.

- Small grains were spherical or sub-spherical in shape and measure approximately 2 μm or less in diameter, rarely reaching sizes larger than 5 μm (not shown).

Cicer arietinum flour consisted of ovoid, rarely spherical simple grains, with the main axis/diameter measuring 10-35 μm; lamellae were more or less visible. The grains had a longitudinal, rather irregular fissure, with short rare transversal secondary fissures; under polarizing l.m., they displayed a bilaterally symmetric cross with a diffuse centre. The grain-size distribution was reported in Fig. S2.

Phytoliths - *Bambusa* contained numerous phytolith morphotypes, differing in shape and size. For the aim of this study, we selected the dumbbell-shaped phytoliths, which were sufficiently large (10-17.5 μm) and easily detectable under l.m.

The different treatments commonly used in the first steps of DNA extraction from ancient dental calculus were proven to only cause negligible effects on the starch grain morphology, while no effect was observed on phytoliths, which appeared unaltered after all of the procedures. The results of the treatments yielded evidence that the "b" and "c" methods caused a loss of the largest starch grains (≥ 20 μm) in both the *Triticum* and *C. arietinum* flour. In contrast, "d" methods caused the loss of the smallest grains. The change in the grain-size distribution was evidenced by a change in the mode of the data set (Fig. S2). Similar results were also observed after the treatments with coupled methods (Figs. S2 and S3). In all the cases, the morphological features of the starch grains did not appear altered when observed both at l.m. and polarizing l.m. Regarding phytoliths, no damage or decrease in their amount was observed.

Globally, the preliminary tests showed that, taking into account some slight losses, the plant materials suffered no appreciable damage during the tested treatments.

2. Combined analyses on ancient dental calculus.

2.1 DNA extraction

An initial qualitative and quantitative analysis was performed on DNA extracted after Procedures A and C. DNA concentration ranged from 33.52 ng/μL to 3.75 ng/μL. Compared to Procedure A, the DNA yield of Procedure C was between 15-31% (Agilent 2100 Bioanalyzer) and 20-47% (QubitTM 4 Fluorometer) lower (S1 Table). Average fragment sizes were in the range of 71 bp and 120 bp, with fragments ranging between 40-200 bp in samples P.O 107-8 and P.O Z. US44 and between 40-800 bp in sample P.O 898-11 (S1 Table). In two samples (P.O 107-8 and P.O Z. US44), fragmentation patterns did not show appreciable variations according to the strategy used, while in sample P.O 898-11, the average fragment length was shorter after Procedure C compared to Procedure A (120 bp and 97 bp, respectively) (S1 Table). Overall, the data showed that both methods are suitable for recovering DNA from dental calculus, but Procedure C causes a loss of genetic material of 28% on average. It was noted that when long DNA molecules were present, as in the sample P.O 898-11, this loss particularly affected the longest fragments.

7

2.2 Analysis of plant microremains.

A small number of phytoliths and starch grains were recovered in all of the calculus samples: the richest content was found in the calculus of individual P.O Z. US44, the poorest in individual P.O 898-11. With the exception of sample P.O 898-11A, phytoliths were always in a smaller amount than starch grains (Fig. S4). With respect to Procedure B, which is the routine method in plant microremain analysis, the decontamination and digestion methods for DNA extraction (Procedures A and C) caused some loss of material, but this loss was not substantial. Regarding starch grains, the lowest values were found after Procedure A in all three samples. On the other hand, a greater variety of phytolith morphotypes was isolated with Procedure A than Procedure C (Table 2).

Cylindric psilate phytoliths were the most common finding in the three individuals (Table 2). Irregularly shaped (i.e., irregular polyhedron) phytoliths were also recorded in P.O Z. US44 and P.O 898-11. Other morphotypes were occasionally recorded. Bulliform, cylindric psylate and prickle phytoliths may refer to the Poaceae family (Fig. 3).

The analysis revealed a low amount of starch grains in all the samples. The greatest portion was rounded or ovoid grains, with centric, closed or linear hilum and extinction crosses with rather straight arms; the diameter/main-axis measured 10-42 μm(morphotype I, Fig. 3) . The grains were often broken or seriously damaged, with visible lamellae, showing a widened extinction cross and a central depression. The grains were generally accompanied by very small grains measuring less than 2.5 μm. These grains may be attributed to *Triticum* and/or *Hordeum* (Fig. 3). Three groups were recorded in samples P.O 108-7 A, P.O Z. US44 B, and P.O 898-11 C. The first group consisted of a few large grains (17-40 μm), similar to those previously described, surrounded by very numerous small grains approximately 2 μm in diameter; the second group was entirely formed by small grains; and the third group was also made of rounded or ovoid grains of different sizes, the largest measuring 7.5-40 μm, with a regular distribution of the size classes (Fig. 3). Numerous small grains (approximately 2.5 μm) were clumped together with the large grains. These groups are also referable to *Triticum* or *Hordeum,* the first group most likely *Hordeum* and the last group mostly likely *Triticum.* In sample P.O 898-11 B, subangular, faceted starch grains were also found (morphotype II, Fig. 3). These grains were approximately 17 μm in size, with centric hilum, deep fissures radiating from the hilum and extinction cross with straight arms. These grains may be attributed to numerous Poaceae, in particular in Panicoideae (millets).

2.3 Metagenomic profiling.

According to the results of the previous analysis on ancient dental calculus (see paragraphs 2.1 and 2.2), DNA extracted from Procedure A was converted into a genomic library and sequenced. After shotgun sequencing, a total of 32,417,928 raw reads were generated (S2 Table). While merged reads obtained from

8

each library were between 1,787,817 and 7,262,574 million, the proportion of reads mapped to the human genome was very low (0.057% for P.O 108-7, 0.046% for P.O Z. US44 and 0.073% for P.O 898-11). No reads mapping to the human mitochondrial genome were detected. These values are in agreement with the human DNA content previously observed in ancient dental calculus (Adler et al. 2013; Mann et al. 2018; Ozga et al. 2016; Warinner et al. 2014a). Cluster factor (ratio of reads before and after PCR duplicate removal) showed a value of 1.00 for each sample (S2 Table). This measure is likely related to the number of PCR cycles carried out during library preparation, and the low rate demonstrates the effectiveness of the protocol used, as well as the high level of complexity of the libraries. Both average fragment length and misincorporation patterns (5' and 3' damage) of the sequences mapped to the human genome were typical of degraded DNA, suggesting a low contamination rates.

Microbial taxonomic profiling (S3 Table) identified a total of 64 genera and 107 species within 9 phyla from the domain *Bacteria* and one phylum from the domain *Archaea*. The most dominant phyla across all the samples were *Firmicutes*, *Actinobacteria*, *Proteobacteria* and *Bacteroidetes*, in different proportions (Fig. S5); these are also the main phyla of the microorganisms inhabiting the human mouth in modern days (Dewhirst et al. 2010). Among the *Archaea*, all the sequences were classified as *Euryarchaeota,* genus *Methanobrevibacter*. The genus *Methanobrevibacter* consists of several species, many of which appear to be specialized to the intestinal tract system of animals (e.g., *M. smithii* in the human gut systems). However, recently, these species have also been identified in human (*M. oralis*) and Neanderthal (*M. oralis* subsp. *neandertalensis*) oral cavities and are associated with periodontal disease (Lepp et al. 2004; Li et al. 2009; Vianna et al. 2009; Weyrich et al. 2017).

The most abundant species identified by our analysis were: *Desulfobulbus sp. oral taxon 041* (21% in P.O 108-7 A, 14.98% in P.O Z. US44 A, 2.35% in P.O 898-11 A); *Lautropia mirabilis* (7.70% in P.O 108-7 A, 14.87% in P.O Z. US44 A, 17.30% in P.O 898-11 A); *Streptococcus sanguinis* (14.68% in P.O 108-7 A, 2.80% in P.O Z. US44 A, 9.49% in P.O 898-11 A); *Propionibacterium propionicum* (4.04% in P.O 108-7 A, 8.49% in P.O Z. US44 A, 1.84% in P.O 898-11 A); *Abiotrophia defectiva* (4.62% in P.O 108-7 A, 2.18% in P.O Z. US44 A, 3.70% in P.O 898-11 A); *Neisseria sicca* (3.40% in P.O 108-7 A, 2.18% in P.O Z. US44 A, 3.95% in P.O 898-11 A). Overall, all the species with > 1% relative abundance, as well as the vast majority of microbial components, were derived from the human oral cavity (Fig. 4, S4 Table, Fig. S6).

Healthy human oral flora contains a large number of endogenous cariogenic, periodontal and opportunistic pathogens. In all the samples, we could detect species associated with dental infections and caries, such as *Porphyromonas gingivalis* (0.14% - 0.25%) and other members of the "red complex" associated with periodontal disease (*Treponema denticola*, 0.44% - 0.63%; and *Tannerella forsythia*, 0.45% - 1.78%) (Fig. 4). It has been shown that these species started to increase in frequency after the transition to agriculture in the early Neolithic period, and they have been strongly associated with periodontal disease during the medieval period, just as they are today (Adler et al. 2013). In addition to the typical oral pathogens, other microorganisms involved in human body infections and disorders (i.e *Propionibacterium* and *Neisseria* species) were observed in our samples (Fig. 4). This observation is consistent with previous studies that have

9

reported that the human oral microbiome includes pathogens that contribute to risk of extraoral disease (Warinner et al. 2014a).

Finally, we observed one species present at substantially high frequencies (ranging between 7.71% and 17.30%) in all the three ancient dental calculus samples: *Lautropia mirabilis* (Fig. 4). While the pathogenicity of *L. mirabilis* in unknown, this bacterium has been identified as a possible agent contributing to dental plaque (Gerner-Smidt et al. 1994). Recent studies showed a possible correlation between *L. mirabilis* abundance and health quality (He et al. 2017; Mok et al. 2017).

It is interesting to note that low percentage of microbial DNA in ancient calculus samples originated from the soil (0.97% for P.O 108-7 A; 8.48% for P.O Z. US44 A; 7.67% in P.O 898-11 A), indicating the efficiency of the decontamination step (Fig. S6).

To verify the authenticity of the oral microbiome, sequences from each sample were then mapped more precisely against the reference genomes of the more abundant oral species (> 1%) listed in S4 Table. Indeed, as reported in S4 Table, the lengths of the mapping reads and their substitution patterns provide important measures of contamination/authenticity. The mean lengths of the reads mapping to bacterial genomes were approximately 42 bp for P.O 108-7 A and P.O Z. US44 A and was 60 bp for P.O 898-11 A (S4 Table). Damage patterns at the ends of the molecules were as would be expected for ancient DNA, ranging from 16.61% to 26.64% for P.O 108-7 A, 18.16% to 23.97% for P.O Z. US44 A and 16.32% to 20.69% for P.O 898-11 A (S4 Table). Overall, these results confirm the ancient origin of the bacterial DNA.

Extraction and library negative controls yielded a total of 32,852 of raw reads. Sequenced reads were processed using the same bioinformatics pipeline applied to the samples. No reads mapping on the human genome were recovered. Regarding the microbial content, the sequences were classified as *Rubrivivax benzoatilyticus*, *Paraburkholderia terrae*, *Xanthomonas perforans* and *Actinomyces* unclassified, and no species of the oral human microbiome were detected.

2.4 Mitochondrial genomes reconstruction.

High throughput sequencing generated 1,254,548 raw reads for sample P.O 108-7, 7,004,204 for P.O Z. US44 and 41.276.132 for P.O 898-11 (S5 Table). We reconstructed the complete or almost complete mitochondrial genome for all the analysed samples, with an average coverage ranging between 9.98% and 109.96%. For samples P.O 108-7 A and P.O Z. US44 A, average fragment length of the post-capture molecules was approximately 10 bp longer than prior to capture, in agreement with previously reported data (Dabney et al. 2013; Ozga et al. 2016). In contrast, P.O 898-11 showed the same length in both pre- and post-capture fragments. After running ContamMix, samples P.O 108-7 A and P.O Z. US44 A revealed high proportions of endogenous DNA (99.81% and 99.43% respectively), while sample P.O 898-11 A showed some degree of contamination that could not be confidently removed even after filtering damaged reads with PMDtools (Skoglund et al. 2014). For non-contaminated samples, mitochondrial lineage was determined using Mitomaster (Brandon et al. 2009): P.O 108-7 A belongs to U5a1c2a1, and P.O Z. US44 A belongs to

X2+225 haplogroup (S5 and S6 Tables). Details of the bioinformatics analysis results can be found in S5 Table.

The results obtained by human mitochondrial DNA capture have further highlighted the effective possibility of performing multiple investigations using a small amount of starting material. Although shotgun results, in agreement with previous studies (Warinner et al. 2014a, 2015), suggest that human DNA is not a substantial component of ancient dental calculus, the capture enrichment strategy (Maricic et al. 2010; Ozga et al. 2016) allowed us to reconstruct complete mitochondrial sequences of two out of three individuals with medium coverage.

Conclusion

In this study we tested different combinations of laboratory procedures to identify the best strategy for simultaneously performing paleogenetic and archaeobotanical analysis on the same sub-sample of tartar. Preliminary tests conducted on fresh plant materials demonstrated that decontamination, decalcification and digestion protocols commonly used to extract aDNA from calcified plaque (Adler et al. 2013; Warinner et al. 2014a) only caused slight losses of microremains and negligible effects on the morphology of the starch grains and phytoliths. When the combined procedures were applied to ancient calculus samples, a decrease in the amount of the recovered phytoliths and starch grains compared to the reference method was generally observed. Despite that, a greater variety of morphotypes was isolated when the residual pellet from the first steps of DNA extraction was directly used for micro-remains analysis (Procedure A). Regarding DNA recovery, the same procedure yielded a concentration 28% higher on average compared with the alternative method (Procedure C). Applying the combined protocol developed here to a set of three medieval samples, we were able to: i. ascertain the use of *Triticum*, *Hordeum* and other Poaceae, possibly including minor cereals, in the diet of a medieval human group from the centre of Rome, ii. achieve high-resolution taxonomic assignments and accurate reconstruction of the oral microbiome's compositional profiles of the three individuals, iii. successfully recover ancient human mitochondrial DNA in two out three of the samples.

The results achieved through the present study have demonstrated the effectiveness of using the same sub-sample of tartar in conducting combined paleogenetic and archaeobotanical analyses reducing the demand of starting material for the interdisciplinary studies. The application of this procedure could therefore overcome the main limiting factors for gathering data, namely, the small amount of tartar preserved on ancient teeth and the importance of retaining some material for further investigations (e.g., paleoproteomic analysis).

11

Ciancio Rossetto for facilitating access to the skeletal materials of the medieval cemetery in the area of *Porticus Octaviae.*

Author contribution

M.L. and M.M.L. conceived the study; A.M., L.P., V.Z., and C.V. performed lab work; M.L., M.M.L., A.M. and E.C. performed data analysis; J.M.C. provided the osteological material and the anthropological interpretation; S.V. and D.C. contributed tools, materials and reagents; M.L., M.M.L. and A.M. wrote the paper with the input of all co-authors.

References

Adler CJ et al. (2013) Sequencing ancient calcified dental plaque shows changes in oral microbiota with dietary shifts of the Neolithic and Industrial revolutions. Nat Genet 45:450-455, 455e451

Brandon MC et al. (2009) MITOMASTER: a bioinformatics tool for the analysis of mitochondrial DNA sequences. Hum Mutat 30:1-6

Briggs AW et al. (2007) Patterns of damage in genomic DNA sequences from a Neandertal. P Natl Acad Sci USA 104:14616-14621

Charlier P, Huynh-Charlier I, Munoz O, Billard M, Brun L, de la Grandmaison GL (2010) The microscopic (optical and SEM) examination of dental calculus deposits (DCD). Potential interest in forensic anthropology of a bio-archaeological method. Leg Med 12:163-171

Ciancio Rossetto P (2008) Portico d'Ottavia - Sant'Angelo in Pescheria: nuove acquisizioni sulle fasi medievali. Rivista di archeologia cristiana 84:415-438

Cristiani E et al. (2018) Dental calculus and isotopes provide direct evidence of fish and plant consumption in Mesolithic Mediterranean. Sci Rep-UK 8:8147

Dabney J et al. (2013) Complete mitochondrial genome sequence of a Middle Pleistocene cave bear reconstructed from ultrashort DNA fragments. P Natl Acad Sci USA 110:15758-15763

Dewhirst FE et al. (2010) The Human Oral Microbiome. J Bacteriol 192(19):5002-17. doi:10.1128/jb.00542-10

Gerner-Smidt P et al. (1994) Lautropia mirabilis gen. nov., sp. nov., a Gram-negative motile coccus with unusual morphology isolated from the human mouth Microbiology 140:1787-1797. doi:doi:10.1099/13500872-140-7-1787

Gilbert MT, Bandelt HJ, Hofreiter M, Barnes I (2005) Assessing ancient DNA studies. Trends Ecol Evol 20:541-544

Hart TC (2011) Evaluating the usefulness of phytoliths and starch grains found on survey artifacts. J Archaeol Sci 38:3244-3253

Hart TC (2016) Issues and directions in phytolith analysis. J Archaeol Sci 68:24-31

He Y, Gong D, Shi C, Shao F, Shi J, Fei J (2017) Dysbiosis of oral buccal mucosa microbiota in patients with oral lichen planus. Oral Diseases 23:674-682. doi:doi:10.1111/odi.12657

Henry AG, Brooks AS, Piperno DR (2014) Plant foods and the dietary ecology of Neanderthals and early modern humans. J Hum Evol 69:44-54

Henry AG, Hudson HF, Piperno DR (2009) Changes in starch grain morphologies from cooking. J Archaeol Sci 36:915-922

Henry AG, Piperno DR (2008) Using plant microfossils from dental calculus to recover human diet: a case study from Tell al-RaqÄ•'i, Syria. J Archaeol Sci 35:1943-1950

Huynh HTT, Verneau J, Levasseur A, Drancourt M, Aboudharam G (2016) Bacteria and archaea paleomicrobiology of the dental calculus: a review. Mol Oral Microbiol 31:234-242 doi:doi:10.1111/omi.12118

Jonsson H, Ginolhac A, Schubert M, Johnson PL, Orlando L (2013) mapDamage2.0: fast approximate Bayesian estimates of ancient DNA damage parameters. Bioinformatics 29:1682-1684

Kircher M, Sawyer S, Meyer M (2012) Double indexing overcomes inaccuracies in multiplex sequencing on the Illumina platform. Nucleic Acids Res. 40(1):e3. doi: 10.1093/nar/gkr771

Kloss-Brandstatter A, Pacher D, Schonherr S, Weissensteiner H, Binna R, Specht G, Kronenberg F (2011) HaploGrep: a fast and reliable algorithm for automatic classification of mitochondrial DNA haplogroups. Hum Mutat 32:25-32

Knights D, Kuczynski J, Charlson ES, Zaneveld J, Mozer MC, et al. (2011) Bayesian community-wide culture-independent microbial source tracking. Nat. Methods 8:761–63

Lazzati AMB, Levrini L, Rampazzi L, Dossi C, Castelletti L, Licata M, Corti C (2016) The Diet of Three Medieval Individuals from Caravate (Varese, Italy). Combined Results of ICP-MS Analysis of Trace Elements and Phytolith Analysis Conducted on Their Dental Calculus. Int J Osteoarchaeol 26:670-681. doi:doi:10.1002/oa.2458

13

Lepp PW, Brinig MM, Ouverney CC, Palm K, Armitage GC, Relman DA (2004) Methanogenic Archaea and human periodontal disease. P Natl Acad Sci USA 101:6176-6181

Li CL et al. (2009) Prevalence and molecular diversity of Archaea in subgingival pockets of periodontitis patients. Oral Microbiol Immunol 24:343-346. doi:doi:10.1111/j.1399-302X.2009.00514.x

Mann AE et al. (2018) Differential preservation of endogenous human and microbial DNA in dental calculus and dentin. Sci Rep-UK 8:9822

Maricic T, Whitten M, Paabo S (2010) Multiplexed DNA sequence capture of mitochondrial genomes using PCR products. PloS one 5:e14004

Mariotti Lippi M, Pisaneschi L, Sarti L, Lari M, Moggi-Cecchi J (2017) Insights into the Copper-Bronze Age diet in Central Italy: Plant microremains in dental calculus from Grotta dello Scoglietto (Southern Tuscany, Italy). J Archaeol Sci: Reports 15:30-39

Meyer M, Kircher M (2010) Illumina Sequencing Library Preparation for Highly Multiplexed Target Capture and Sequencing. Cold Spring Harbor Protocols 2010:pdb.prot5448 doi:10.1101/pdb.prot5448

Modi A et al. (2017) Complete mitochondrial sequences from Mesolithic Sardinia. Sci Rep-UK 7:42869

Mok S, Karuthan C, Cheah Y, Ngeow W, Rosnah Z, Yap S, Ong H (2017) The oral microbiome community variations associated with normal, potentially malignant disorders and malignant lesions of the oral cavity. Malays J Pathol 39:1-15

O'Regan HJ, Lamb AL, Wilkinson DM (2016) The missing mushrooms: Searching for fungi in ancient human dietary analysis. J Archaeol Sci 75:139-143

Ozga AT et al. (2016) Successful enrichment and recovery of whole mitochondrial genomes from ancient human dental calculus. Am J Phys Anthropol 160:220-228. doi:doi:10.1002/ajpa.22960

Peltzer A, Jager G, Herbig A, Seitz A, Kniep C, Krause J, Nieselt K (2016) EAGER: efficient ancient genome reconstruction. Genome Biol 17:60

Piperno DR (2006) Phytoliths: a Comprehensive Guide for Archaeologists and Paleoecologists. AltaMira Press, Lanham, Maryland

Radini A, Buckley S, Rosas A, Estalrrich A, de la Rasilla M, Hardy K (2016) Neanderthals, trees and dental calculus: new evidence from El Sidron. Antiquity 90:290-301

Radini A, Nikita E, Buckley S, Copeland L, K H (2017) Beyond food: The multiple pathways for inclusion of materials into ancient dental calculus. Am J Phys Anthropol 162:71-83

Rusu I et al. (2018) Dual DNA-protein extraction from human archeological remains. Archaeol Anthrop Sci. doi:10.1007/s12520-018-0760-1

Scott GR, Poulson SR (2012) Stable carbon and nitrogen isotopes of human dental calculus: a potentially new non-destructive proxy for paleodietary analysis. J Archaeol Sci 39:1388-1393

Seidemann J (1966) Starke-Atlas. Grundlagen der Starke-Mikroskopie und Beschreibung der wichtigsten Starkearten vol 19. vol 11. Verlag Paul Parey, Berlin. doi:doi:10.1002/star.19670191108

Skoglund P, Northoff BH, Shunkov MV, Derevianko AP, Paabo S, Krause J, Jakobsson M (2014) Separating endogenous ancient DNA from modern day contamination in a Siberian Neandertal. P Natl Acad Sci USA 111:2229-2234

Soncin S, Hendy JR, Speller CF, Manzi G, Tafuri M (2016) Diet and Health in Middle Bronze Age Italy: a metaproteomic analysis of human dental calculus in two case-studies. Paper presented at the IMEKO International Conference on Metrology for Archaeology and Cultural Heritage, Torino, Italy,

Truong DT et al. (2015) MetaPhlAn2 for enhanced metagenomic taxonomic profiling. Nat Met 12:902-903

van Oven M, Kayser M (2009) Updated comprehensive phylogenetic tree of global human mitochondrial DNA variation. Hum Mutat 30:E386-394

Varalli A, Moggi-Cecchi J, Moroni A, Goude G (2015) Dietary Variability During Bronze Age in Central Italy: First Results International Journal of Osteoarchaeology 26:431-446 doi:doi:10.1002/oa.2434

Vianna ME, Conrads G, Gomes BPFA, Horz HP (2009) T-RFLP-based mcrA gene analysis of methanogenic archaea in association with oral infections and evidence of a novel Methanobrevibacter phylotype. Oral Microbiol Immunol 24:417-422. doi:doi:10.1111/j.1399-302X.2009.00539.x

Wang TT, Fuller BT, Wei D, Chang XE, Hu YW (2015) Investigating Dietary Patterns with Stable Isotope Ratios of Collagen and Starch Grain Analysis of Dental Calculus at the Iron Age Cemetery Site of Heigouliang, Xinjiang, China. Int J Osteoarchaeol 26:693-704. doi:doi:10.1002/oa.2467

14

Warinner C et al. (2014a) Pathogens and host immunity in the ancient human oral cavity. Nat Genet 46:336-344

Warinner C et al. (2014b) Direct evidence of milk consumption from ancient human dental calculus Sci Rep-UK 4:7104

Warinner C, Speller C, Collins MJ (2015) A new era in palaeomicrobiology: prospects for ancient dental calculus as a long-term record of the human oral microbiome Philos T R Soc Lond 370:20130376

Warinner C, Herbig A, Mann A, Fellows Yates JA, Weiß CL, Burbano HA, Orlando L, Krause J (2017) A Robust Framework for Microbial Archaeology. Annu Rev Genomics Hum Genet. 18:321-356. doi: 10.1146/annurev-genom-091416-035526

Weyrich LS, Dobney K, Cooper A (2015) Ancient DNA analysis of dental calculus. J Hum Evol 79:119-124

Weyrich LS et al. (2017) Neanderthal behaviour, diet, and disease inferred from ancient DNA in dental calculus. Nature 544:357

Willerslev E, Cooper A (2005) Ancient DNA. Proc R Soc Lond [Biol] 272: 3-16. doi:708 10.1098/rspb.2004.2813.

1
2
3
4
5
6
7
8
9
10
11
12
13
14
15
16
17
18
19
20
21
22
23
24
25
26
27
28
29
30
31
32
33
34
35
36
37
38
39
40
41
42
43
44
45
46
47
48
49
50
51
52
53
54
55
56
57
58
59
60
61
62
63
64
65

Tables

Sample ID	Tooth	Weight (mg)	Total weight (mg)	Quantity used for each procedure (mg)
P.O 108-7	M_1 sx	22	77	A, 22
	M_2 dx	32		B, 23
	P_2 dx	23		C, 22
P.O Z. US44	P^2 sx	7	38	A, 13
	P^1 dx	10		B, 11
	M^1 sx	21		C, 12
P.O 898-11	I_1 dx	37	108	A, 32
	I_1 sx	67		B, 34
	C_1 dx	4		C, 31

Table 1: Sampling of the dental calculus. For each sample, tooth sampled, weight of calculus recovered from each tooth, total weight collected and quantity of calculus used for different procedures are reported.

Morphotypes	P.O 108-7			P.O Z. US44			P.O 898-11		
	A	B	C	A	B	C	A	B	C
Armed hair cell		1							
Bulliform		1			1			1	
Cylindric psylate perfectly paralleledipedal				2			1		
Cylindric psylate with short basis oblique		5	4	5	1		2	3	
Elongate echinate					1				
Tissue fragments					1				
Orbiculare		1		2		1			
Irregular shaped				7	6	8		4	3
Prickle					1				
Scrobiculate epidermal cell	3	3			2		1		5
Spherical scalloped					1				
Vessels	1	1				1			
Tracheids							1		
Trapeziform sinuate	1	1			4				

Table 2. Quantitative analysis results of the silicified plant microremains. For each sample, the number of morphotypes recovered after Procedures A, B and C is reported.

Figures
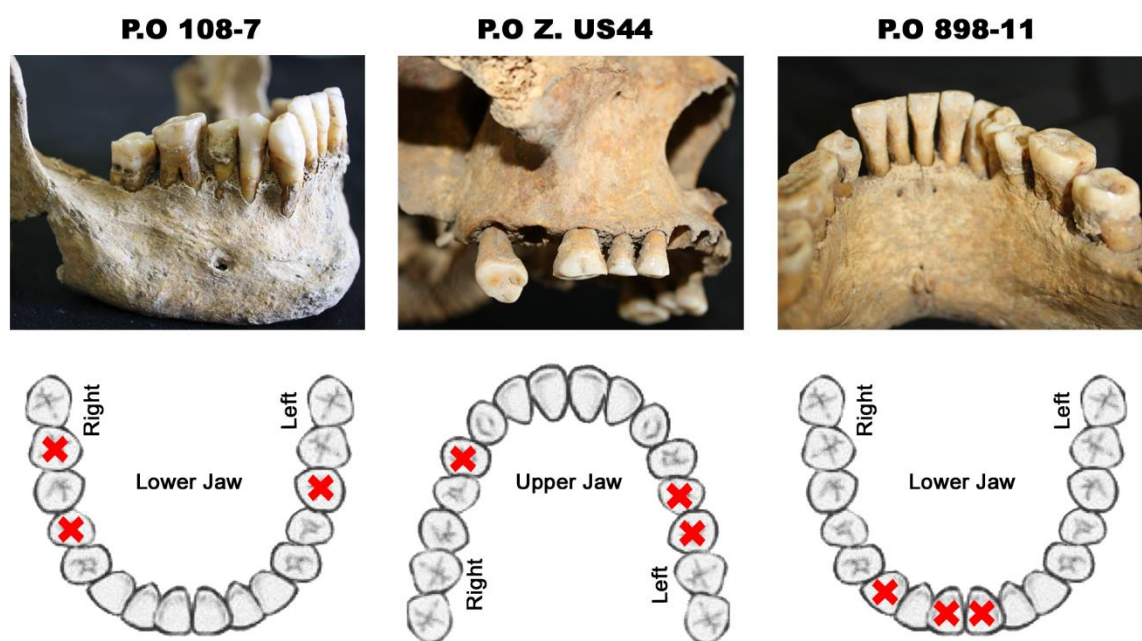
Fig. 1. Human dental material from Porticus Octaviae (Rome, Italy), with indication of the teeth sampled for dental calculus (red crosses).
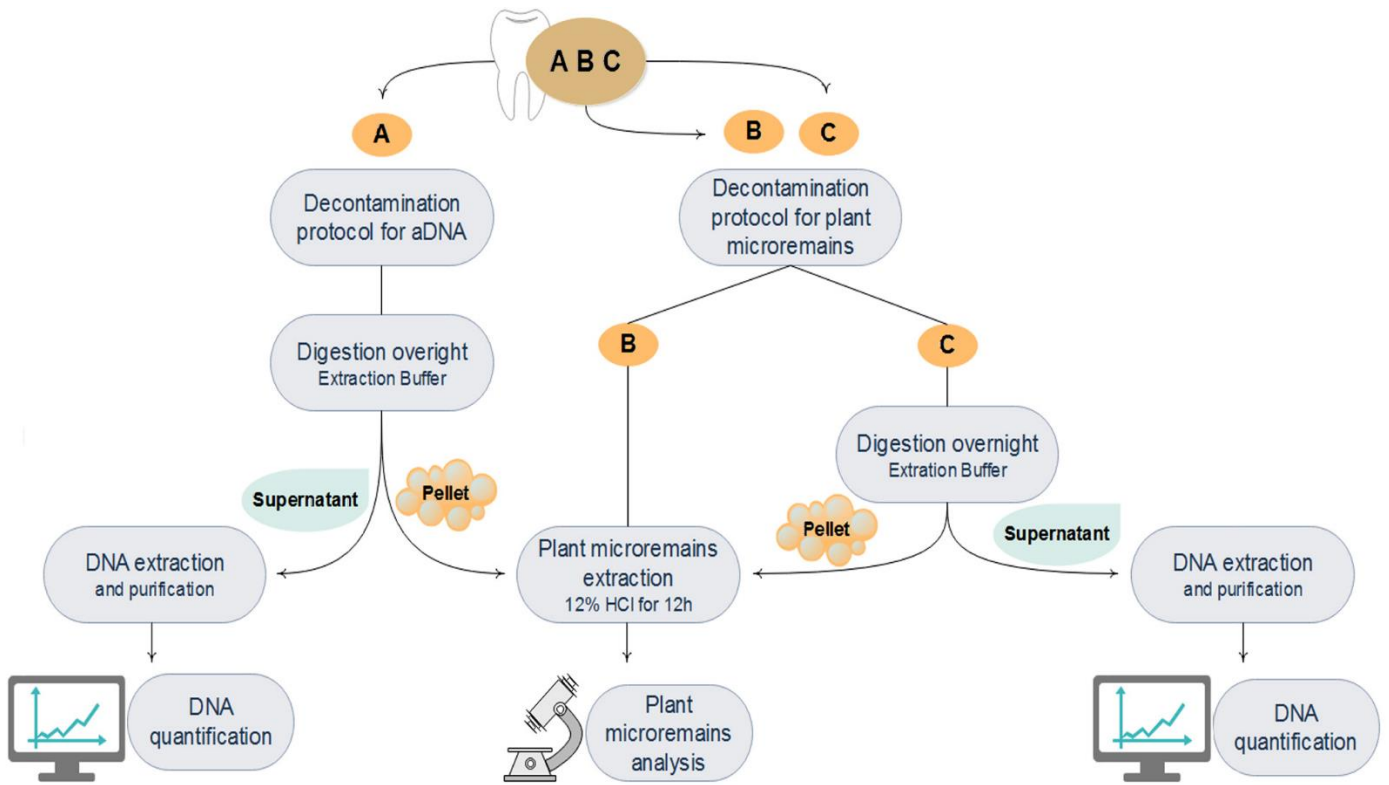
Fig. 2. Overview of the experimental design followed for testing the combined procedures.
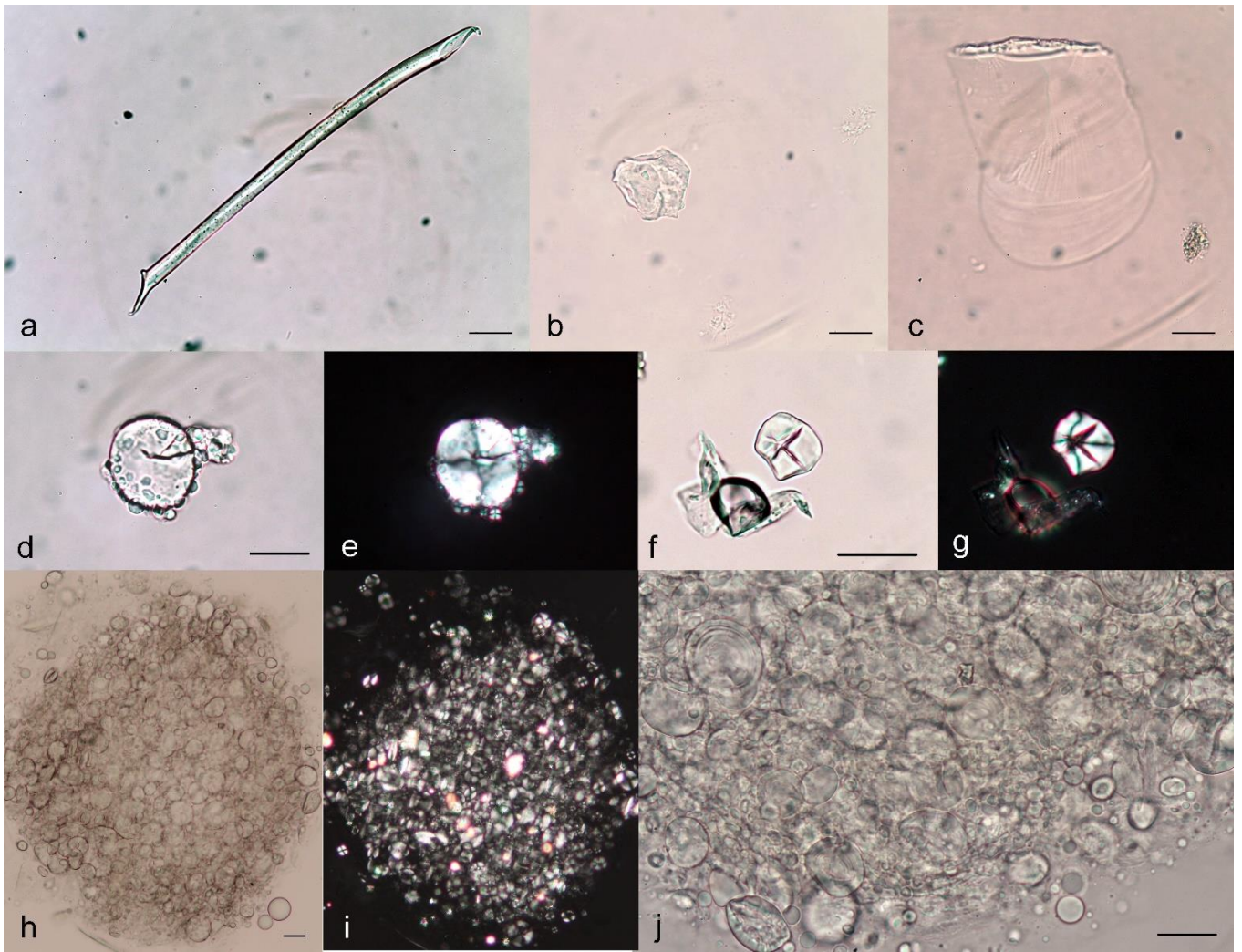
Fig. 3. Phytoliths and starch grains from the calculus deposit recovered in the ancient samples of Porticus Octaviae under l.m. a-c) Phytoliths: a) cylindric psilate; b) irregular; c) bulliform. d-j) Starch grains: d) morphotype I; e) the same under polarizing l.m.; f) morphotype II; g) the same under polarizing l.m.; h) a large starch grain clustered together with numerous smaller grains; i) the same group under polarizing l.m.; j) a detail of the same group at greater magnification. Bar = 20 μm

Bacteroidetes_oral_taxon_274
Propionibacterium_propionicum
Eikenella_corrodens
Bacteroidetes_bacterium_oral_taxon_272
Treponema_socranskii
Corynebacterium_matruchotii
candidate_division_TM7_single_cell_isolate_TM7c
Prevotella_loescheii
Actinomyces_oris
candidate_division_TM7_single_cell_isolate_TM7b
Eubacterium_saphenum
Fretibacterium_fastidiosum
Actinomyces_cardiffensis
Treponema_denticola
Capnocytophaga_gingivalis
Neisseria_macacae
Eubacterium_yurii
Campylobacter_showae
Tannerella_forsythia
Neisseria_sicca
Abiotrophia_defectiva
Neisseria_elongata
Lachnospiraceae_oral_taxon_107
Capnocytophaga_sp_oral_taxon_329
Peptostreptococcus_stomatis
Corynebacterium_durum
Aggregatibacter_aphrophilus
Rothia_aeria
Cardiobacterium_hominis
Selenomonas_noxia
Actinomyces_johnsonii
Prevotella_saccharolytica
Johnsonella_ignava
Gemella_morbillorum
Cardiobacterium_valvarum
Streptococcus_gordonii
Pyramidobacter_piscolens
Campylobacter_rectus
Prevotella_intermedia
Campylobacter_gracilis
Olsenella_uli
Catonella_morbi
Fusobacterium_nucleatum
Filifactor_alocis
Kingella_denitrificans
Aggregatibacter_segnis
Granulicatella_adiacens
Neisseria_flavescens
Streptococcus_oligofermentans
Streptococcus_cristatus
Treponema_maltophilum
Actinomyces_viscosus
Actinomyces_naeslundii
Capnocytophaga_granulosa
Porphyromonas_gingivalis
Lachnospiraceae_bacterium_ICM7
Rothia_dentocariosa
Actinomyces_odontolyticus
Veillonella_parvula
Pseudoramibacter_alactolyticus
Haemophilus_parainfluenzae
Prevotella_maculosa
Candidatus_Prevotella_conceptionensis
Streptococcus_constellatus
Actinomyces_georgiae
Oribacterium_sp_oral_taxon_078
Parvimonas_micra
Eubacterium_infirmum
Capnocytophaga_ochracea
Desulfovibrio_desulfuricans
Selenomonas_sputigena
Eubacterium_brachy
Selenomonas_infelix
Actinomyces_massiliensis
Dialister_invisus
Centipeda_periodontii
Porphyromonas_catoniae
Streptococcus_anginosus
Porphyromonas_endodontalis
Slackia_exigua
Prevotella_micans
Anaeroglobus_geminatus
Leptotrichia_buccalis
Streptococcus_infantis
Olsenella_profusa
Vicia_cryptic_virus
Rothia_mucilaginosa
Fusobacterium_periodonticum
Eggerthia_catenaformis
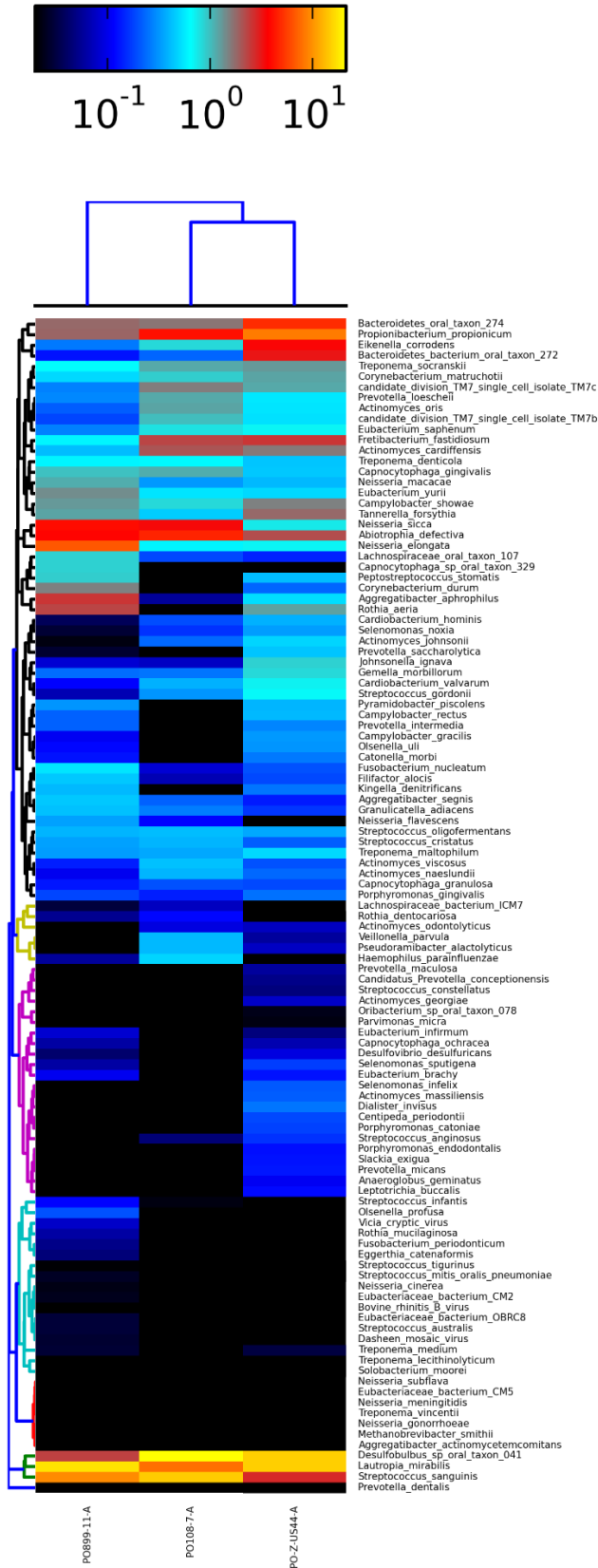Streptococcus_tigurinus
Streptococcus_mitis_oralis_pneumoniae
Neisseria_cinerea
Eubacteriaceae_bacterium_CM2
Bovine_rhinitis_B_virus
Eubacteriaceae_bacterium_OBRC8
Streptococcus_australis
Dasheen_mosaic_virus
Treponema_medium
Treponema_lecithinolyticum
Solobacterium_moorei
Neisseria_subflava
Eubacteriaceae_bacterium_CM5
Neisseria_meningitidis
Treponema_vincentii
Neisseria_gonorrhoeae
Methanobrevibacter_smithii
Aggregatibacter_actinomycetemcomitans
Desulfobulbus_sp_oral_taxon_041
Lautropia_mirabilis
Streptococcus_sanguinis
Prevotella_dentalis

10^{-1} 10^{0} 10^{1}

P0899-11-A
PO108-7-A
PO-Z-US44-A

Fig. 4. Heatmap of the microbial community inferred by MethaPhlan2 (Truong et al. 2015) from shotgun data of ancient dental calculus. Species-level taxonomic profiles of all the clades, hierarchically clustered with the Bray-Curtis similarity, are reported for the three samples of Porticus Octaviae.

Figures

	DECALCIFICATION / DIGESTION METHODS		
	c	d	e
DECONTAMINATION METHODS a	a+c	a+d	a+e
DECONTAMINATION METHODS b	b+c	b+d	b+e

S1 Fig. Summary of the different assays of decontamination and/or decalcification/digestion tested on fresh plant materials. a and b, decontamination methods; c, d and e, decalcification and digestion methods.
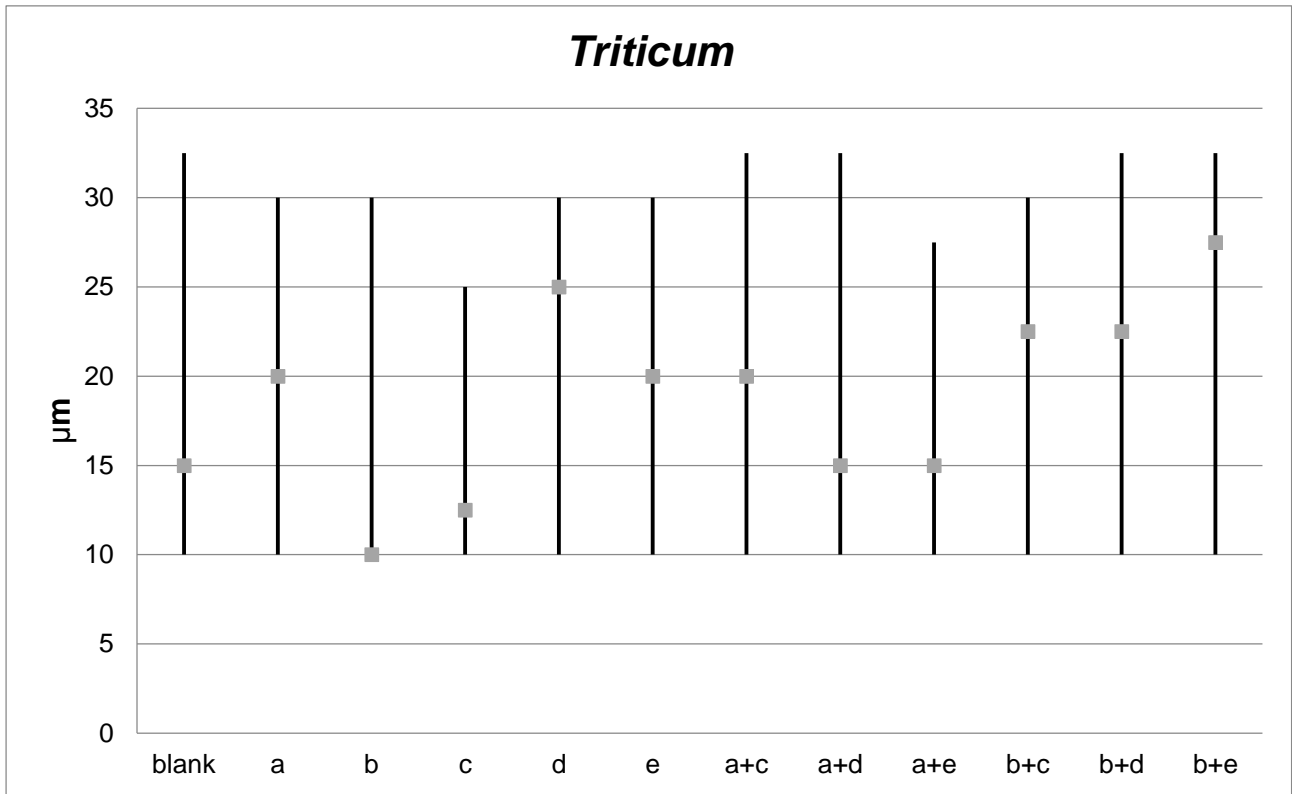
S2 Fig. Size distribution (min, max and mode) of the *Triticum* and *Cicer* starch grains before and after the processing methods.
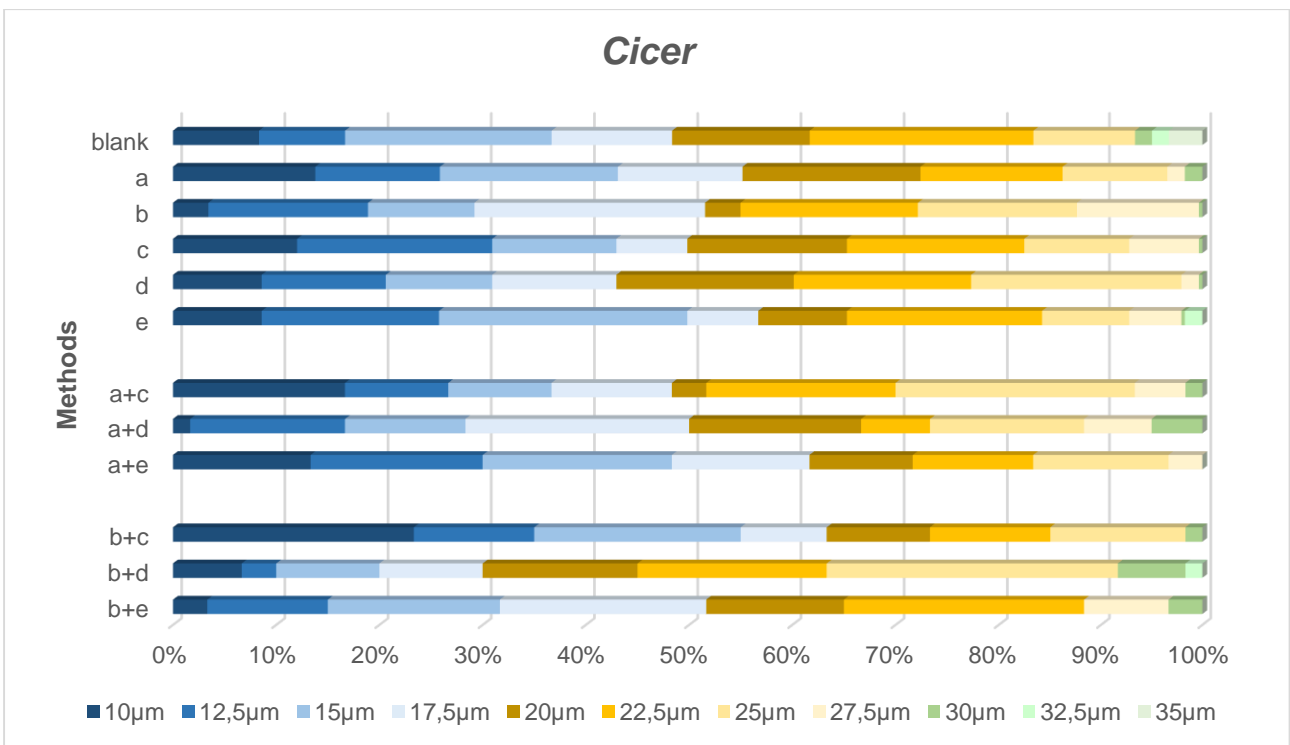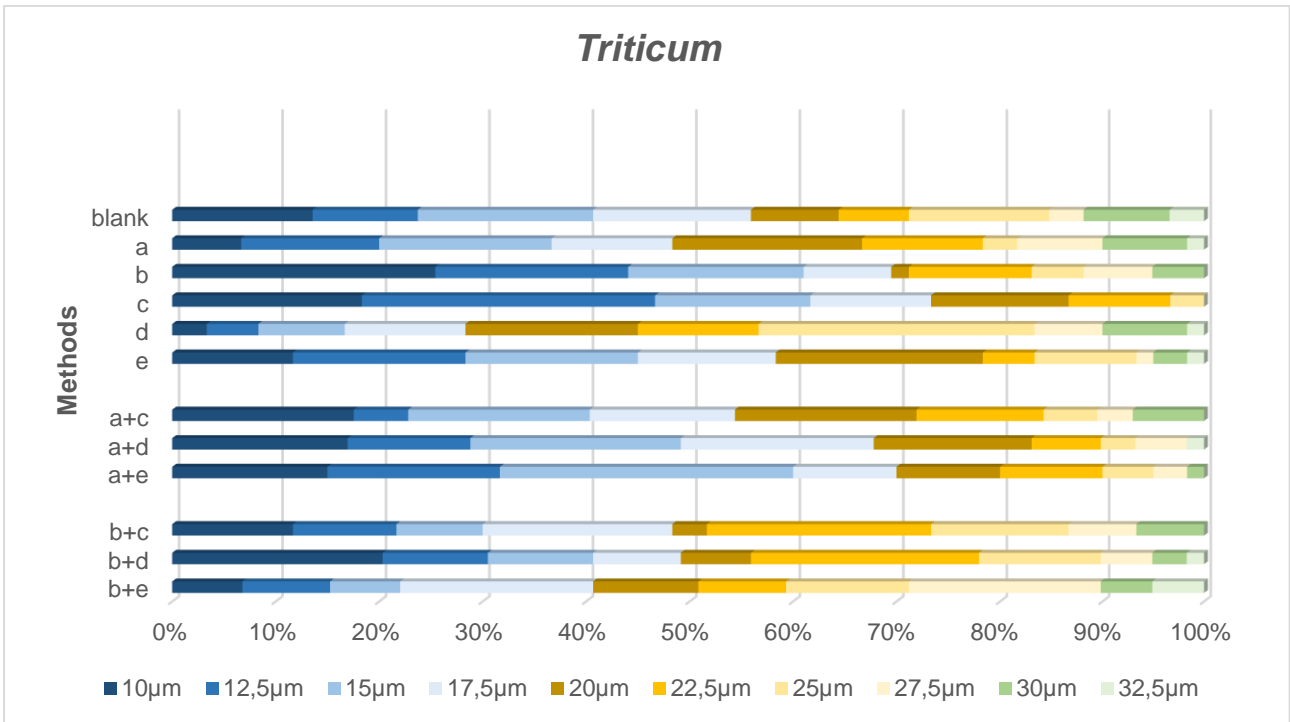
S3 Fig. Bar plots of size distribution of *Triticum* and *Cicer* starch grains before and after the processing methods.
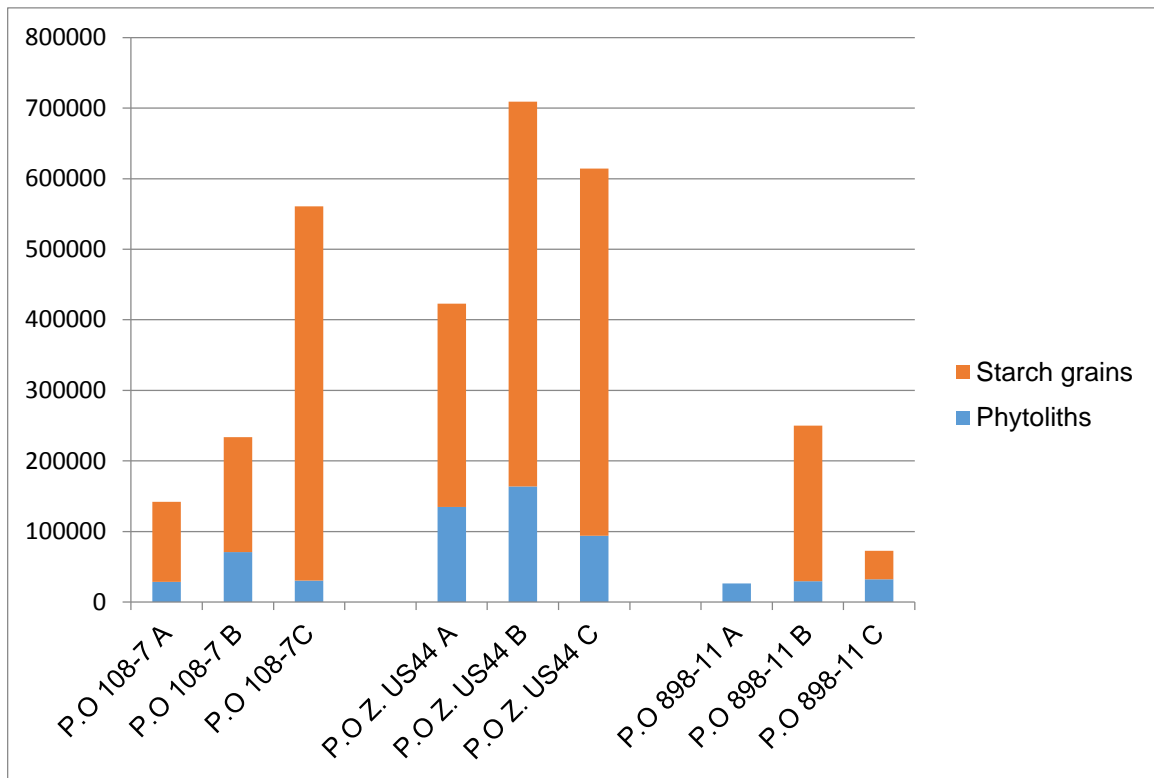
S4 Fig. Phytolith and starch grain concentration (records for gram) in the examined subsamples.
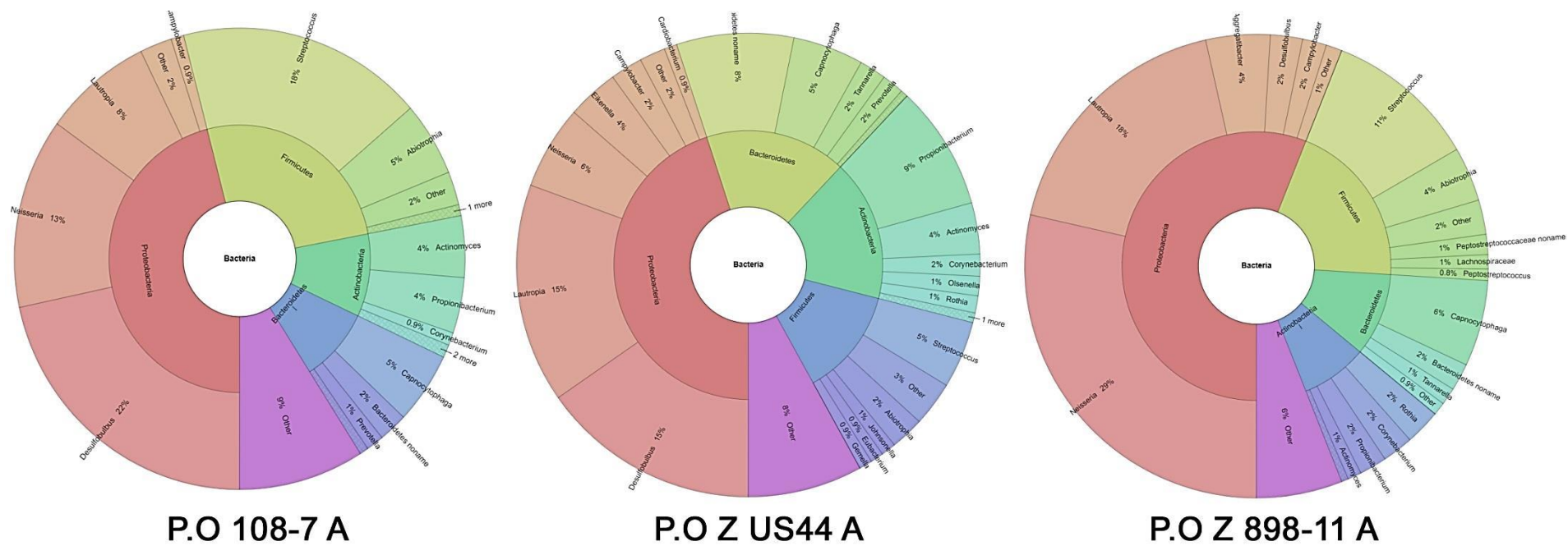
S5 Fig. Representation of microbial composition at the phylum level from Krona graphs for the three analysed ancient samples. Phyla with relative abundance < 5% are labelled together as "other"
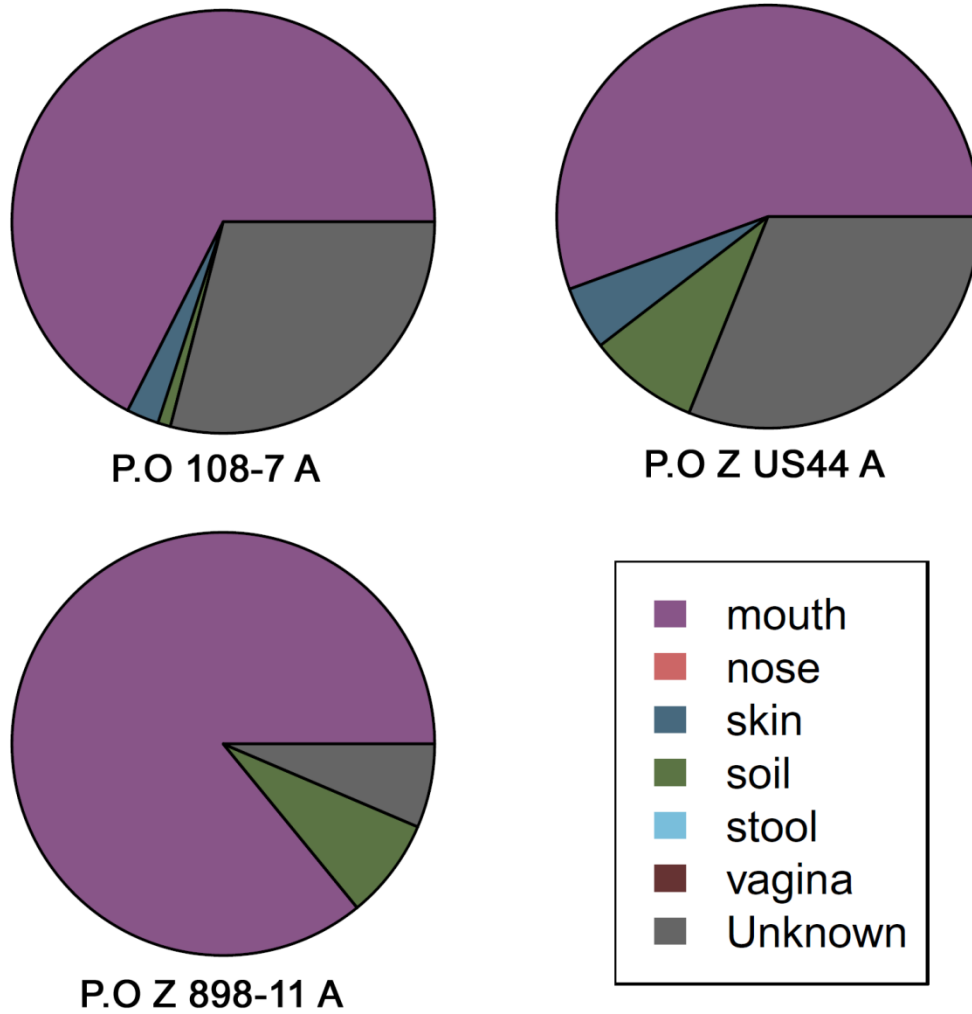
S6 Fig. Bayesian source estimation of the microbial composition of ancient dental calculus using SourceTracker (Knights et al., 2011)

Archaeological and Anthropological information

Notes on the archaeological site. The Portico of Octavia (Porticus Octaviae) was built in the period between 27 and 23 BC from Augustus, and derives its name from being dedicated by Augustus to his sister Octavia. The Church of Sant'Angelo in Pescheria was built in the same area around 750 AD. The cemetery is located in front of the church and it is the most important medieval necropolis in the urban area of Rome, with over 30 tombs, the vast majority of which are multiple burials. The use of the cemetery area extends from the 9th to the 13th century, with a phase that includes the high Middle Ages and one that goes from the 11th century to its abandonment in the 13th century. Two human bone fragments from US 898 were radiometrically dated to a period between 950 AD and 1030 AD. The cemetery area has been the subject of various excavation campaigns: in 1996-1997, in 2000-2002 and finally in 2010. The finds considered here were excavated in 2001. The ditches identified are both earthy and caisson, the latter usually lined in bricks; there are mainly multiple burials which in some cases represent real ossuaries. The samples analyzed come from ossuaries, so it was not possible to associate the cranial findings with the corresponding postcranial findings. After excavation no cleaning, restoration, or handling without protections were performed on the remains analyzed in this study.

Anthropological notes on the human remains. Three specimens have been analyzed. No skeletal or dental evidence of pathology or disease is present.

1) P.O 108-7 is an isolated mandible, belonging to an adult individual possibly male. Overall conditions of the dentition are good. Ante mortem loss of left M1 is evident. Dental wear is mild. Retraction of the alveolar margin is present.

2) P.O Z. US44 is an isolated mandible, belonging to an adult individual possibly male. Overall conditions of the dentition are good. Dental wear is mild. Retraction of the alveolar margin is evident. Light linear enamel hypoplasia is present on the right Canine.

P.O 898-11 is a calvarium, belonging to an adult individual possibly male. Overall conditions of the skull and of the dentition are good. Dental wear is mild/marked. Retraction of the alveolar margin is evident. Light linear enamel hypoplasia is present on the left canine, P1 and P2.

Preliminary tests on fresh plant materials

Fresh plant materials were analyzed in the Laboratory of Plant Biology, University of Florence. Starch grains were obtained from the flour of wheat (*Triticum aestivum* L.) and chickpeas (*Cicer arietinum*). Twenty mg of each sample of starch grains were resuspended in 1 ml of biomolecular grade water (ddH$_2$O) in a 2 ml

Eppedorf tube. Phytoliths were isolated from bamboo (*Bambusa sp.*) leaves collected in the Botanical Garden of the University of Florence, using two different methods:

1) *Dry ashing* (ASH). The dry ashing method utilizes the high temperatures to extract phytoliths. 3 leaves were fragmented, dehydrated at 60°C for 3 days in oven and then heated in muffle furnace at 500°C for 2 hours. The ashed sample was treated with 65% HNO_3 solution for 30 minutes. Afterwards, the residue was washed with hot water and resuspended in 0.5 ml of 50% v/v water-glycerol solution.

2) *Wet Oxidation* (WET). The wet oxidation method uses a cocktail of different mineral acids to digest the plant material. After fragmentation, 3 leaves were autoclaved twice, first at 110°C for 1 hour with distilled water and then at 120°C for 2 hours with 7% NaOH water solution. Pre-digested materials were sifted at 50 μm, washed with hot water and treated with 65% HNO_3 solution for 30 minutes. After decantation the residue was washed with hot water and resuspended in 0.5 ml of 50% v/v glycerol solution.

Decontamination methods. Two different decontamination methods were tested on fresh plant materials (starch grains and phytolithis) (Fig. S1):

Method a. One ml of 1% NaOCl solution was added to 100 μl of fresh plant materials, stood for 1 minute and then washed 3 times to pH neutrality with 1 ml of biomolecular grade water. After the third wash, the plant materials were divided into 4 aliquots: 3 aliquots were resuspended in 100 μl of ddH_2O and used for the decalcification and digestion step described below; 1 aliquot was resuspended in 300 μl of 50% v/v glycerol solution and used for testing the effects of decontamination method a.

Method b. One ml of 0.5 M EDTA was added to 100 μl of fresh plant materials, stood for 1 hour and then EDTA solution was removed. Plant materials were washed tree time and were divided into 4 aliquots and used as described above.

Decalcification and pre-extraction digestion methods. Three digestion methods were tested on different aliquots of both decontaminated (method "a" and method "b") and non-decontaminated plant materials for 9 different assays globally (Fig. S1):

Method c. Hundred μl of plant materials was digested overnight at 55°C in 1 mL of Extraction Buffer, comprised of 0.45 M EDTA, 0.25 mg/ml Proteinase K and 0.05% Tween 20, on a rotary mixer. After pelleting, Extraction Buffer was removed and the plant materials were resuspended in 100 μl of 50% v/v water-glycerol solution.

Method d. Hundred μl of plant materials was digested in 1 mL of 0.5 M EDTA for 24 hours at room temperature on a rotary mixer. After pelleting, EDTA was removed and the plant materials were resuspended in 100 μl of 50% v/v water-glycerol solution.

<u>Method e</u>. Hundred μl of plant materials was digested overnight at 55°C in 1 mL of Extraction Buffer followed by 24 hours digestion at room temperature on a rotary mixer. After pelleting, EDTA was removed and the plant materials were resuspended in 100 μl of 50% v/v water-glycerol solution.

To determine the possible effects of the decontamination and the decalcification/digestion methods on morphological features and on total yield of the starch grains and phytoliths, the untreated and treated materials (11 different assays, Fig. S1) were examined under a l.m and polarizing l.m.

Comparison of different procedure for the analysis of ancient dental calculus

Ancient dental calculus was collected from human teeth using a sterilized dental scalar. The sampling was conducted in the clean-room facilities of the Laboratory of Molecular Anthropology and Paleogenetics, University of Florence, using protective clothing, face mask and gloves to avoid DNA contamination. Before removal, the surface of the calculus was cleaned using a bleach-sterilized brush and UV irradiated (250 nm) for 10 min.

For individual P.O 108-7, calculus was collected from lower left M1, lower right M2 and P2, yielding a total of 77 mg. For individual P.O Z. US44, calculus was removed from upper right P1, upper left P2 and M1, obtaining a total of 38 mg. For individual P.O 898-11, calculus was sampled from lower left I1, right I1 and C, yielding a total of 108 mg (Fig. 1 and Table 1). Calculus collected from each individual was combined into a single tube, coarsely ground with a sterile micropestel, divided into three sub-samples of approximately the same weight and processed according the following procedures (Fig. 2).

<u>PROCEDURE A</u>. Dental calculus was soaked in 1 ml of 0.5 M EDTA, vortexed and incubated at room temperature for 1 minute to remove environmental contaminants. After centrifuge at 13.000 rpm for 3 minutes, EDTA was removed and the sample was crushed in order to obtain a coarse powder that was subsequently digested overnight at 37°C in 1 ml of Extraction Buffer (0.45 M EDTA, 0.25 mg/ml Proteinase K and 0.05% Tween 20). After pelleting, pellet was used for plant microremains extraction (Henry and Piperno, 2008; see Procedure B) and the supernatant was extracted as described in Dabney et al. (2013). DNA was isolated and purified on MinElute column (Qiagen) and eluted twice in a final volume of 100 μl of EB buffer. DNA yield was quantified using Agilent 2100 Bioanalyzer with High Sensitivity DNA chip and Qubit[TM] 4 Fluorometer (dsDNA High Sensitivity Kit).

<u>PROCEDURE B</u>. In order to remove the surface contaminants, dental calculus was treated according to Henry and Piperno (2008). Each sample was boiled in water for 1 minute and, after centrifuge at 2000 rpm for 7 minutes, pellet was resuspended in 10% sodium hexametaphosphate water-solution to deflocculate the calculus. After 24 hours, the sample was sonicated for 5 minutes, centrifuged at 2000 rpm for 2 minutes and the pellet was washed two times with distilled water and rinsed in 10% HCl solution for 12 hours. The

calculus was finally rinsed twice in distilled water and stored in 5 mL of 50% v/v glycerol solution (Henry and Piperno 2008).

PROCEDURE C. Dental calculus was decontaminated as described in Procedure B: each sample was boiled in distilled water for 1 minute and, after centrifugation, rinsed in 10% sodium hexametaphosphate solution for 24 hours. Sample was then sonicated and washed two times with distilled water (Henry and Piperno 2008). The resulting pellet was digested overnight at 37°C in 1 ml of Extraction Buffer (0.45 M EDTA, 0.25 mg/ml Proteinase K and 0.05% Tween 20). After centrifugation, the supernatant was used for DNA extraction as described in Procedure A. DNA yield was quantified using Agilent 2100 Bioanalyzer with High Sensitivity DNA chip and Qubit™ 4 Fluorometer (dsDNA High Sensitivity Kit). The pellet, instead, was incubated in HCl 10% for 12 hours rinsed twice in distilled water and resuspended in 5 mL of 50% v/v water-glycerol solution.

Plant microremains analysis on ancient dental calculus

After plant microremains isolation in Procedure A, B and C, sub-samples were mounted on microscope slides (10 µl for each slide) and examined under a l.m. and polarizing l.m (operating at 400 magnification) to observe starch grains and phytoliths. Starch grains were classified according to their morphology and identified on the basis of literature (Henry et al. 2009; Piperno 2006; Seidemann 1966) and reference collections. For phytoliths, classification was carried out on the basis of their anatomical origin, where possible, or grouping them according to the geometrical shape. The terminology followed Madella et al. (2005, 2016) and Piperno (2006).

To verifying the occurrence of a possible contamination in analyzed ancient dental calculus, for each sample, a surface of about 3-5 cm^2 of the frontal bone (P.O Z. US44) or mandible (P.O 108-7 and P.O 898-11) was washed with distilled water brushing the area with a sterilized brush (Mariotti Lippi et al. 2017). Ten µl of the control samples were examined under a l.m. and polarizing l.m. and compared with the observations from dental calculus. While phytoliths and starch grains were recovered in all of the calculus samples, all the controls resulted negative.

Bioinformatic analysis

Shotgun data. Raw reads were demultiplexed according to sample specific index sequences and then analyzed using a bioinformatics pipeline specific for ancient DNA samples. FastQC software (https://www.bioinformatics.babraham.ac.uk/projects/fastqc/) was used for read quality control. Adapter sequences were trimmed and paired-end reads with a minimum overlap of 10 bp were collapsed using Clip&Merge v. 1.7.4 (Peltzer et al. 2016) and then treated as single-end reads. Reads with length < 30 bp

were discarded. Filtered reads were mapped to the human reference genome (Hg19, NCBI Build 38, December 2017) using BWA v. 0.7.10 (Li and Durbin 2009) with seeding disabled (-l 1000) and edit distance increased (-n 0.01) (Schubert et al. 2012). Only reads with a mapping quality higher than 30 were kept. DeDup was used to remove PCR duplicates and cluster factor value was taken into account to evaluate the effectiveness of the protocol used to enrich libraries. Damage patterns were assessed using MapDamage 2.0 (Jonsson et al. 2013).

Microbial communities were profiled using MetaPhlan2 (Truong et al. 2015). Non-human reads were mapped to the clade-specific marker sequences database in MetaPhlan using Bowtie2 v. 2.3.3 aligner (Langmead and Salzberg 2012) setting default parameters. Microorganism taxonomic groups and their relative abundances were determined for each taxonomic level. For each sample, relative abundances at the phylum and genus levels were visualized by interactive pie charts (Fig. S5) created using Krona tool v. 2.4 (Ondov et al. 2011). Hierarchal clustering analysis was carried out at species-level and described by a heatmap generated with Hclust2 (Warnes et al. 2015). Bray-Curtis index was used as the distance measure between both samples and microorganisms (Fig. 4).

The authenticity of the oral microbiome was established by deamination and length patterns analysis (S3 Table). For each sample, reads were aligned with the reference sequences of the most abundant oral species (> 1%) (S3 Table) using CircularMapper (BWA parameters: -n 0.02, -l 1000) in order to take into account the circularity of the bacterial genomes (Peltzer et al. 2016). Duplicates were removed using DeDup (Peltzer et al. 2016) and reads with a mapping quality lower than 30 were discarded. Ancient DNA damage patterns were assessed using MapDamage2 (Jonsson et al. 2013).

In addition to deamination and fragmentation patterns, Bayesian source estimation was used for authentication of the microbial profile obtained for each sample (Warinner et al. 2017). Using SourceTracker (Knights et al., 2011), we compared dental calculus data to a metagenomic dataset (Louvel et al. 2016) consist of samples from mouth (N = 382), skin (N = 11), nose (N = 81), vagina (N = 45) and stools (N = 127) published in Human Microbiome Project Consortium (2012) and from soil (N = 15) (Der Sarkissian et al. 2014) likely to be sources of contaminants (Fig. S6).

Mitochondrial genome reconstruction and authentication. After demultiplexing, enriched libraries were analyzed using a pipeline specific for ancient DNA. EAGER (Peltzer et al. 2016) was used for initial quality control, adapter trimming and merging paired-end reads. Reads with < 30 bp length were discarded. Filtered reads were mapped to the Revised Cambridge Reference Sequence (rCRS, NC_012920.1) using CirculaMapper (BWA parameters: -n 0.02, -l 1000 to improve accuracy of ancient DNA reads, as recommended in Schubert et al. (2012)) a tool integrated in EAGER designed for circular reference genomes. Endogenous ancient DNA fragments were then separated from contaminating sequences possibly present in the molecules sequenced, using PMDtools (setting pmdscore $\geq$3), a likelihood approach that takes into account postmortem degradation at the ends of the sequences (Skoglund et al. 2014). Before to

reconstruct the consensus sequences, 5 bases of each end of the damaged reads were trimmed to reduce the error rate due to deamination. MtDNA sequences were assembled using mpileup and vcfutils.pl of the SAMtools package (Li and Durbin 2009). Consensus sequence was called for nucleotide positions covered by at least two reads. For each consensus sequence, contamination level was estimated by ContamMix (Fu et al. 2013) a Bayesian-based tool that evaluates the probability that a given read derived from a contaminant source; a set of 311 present-day human mitochondrial genomes was used as possible contamination source.

References

Dabney J et al. (2013) Complete mitochondrial genome sequence of a Middle Pleistocene cave bear reconstructed from ultrashort DNA fragments. P Natl Acad Sci USA 110:15758-15763

Der Sarkissian C, Ermini L, Jonsson H et al. (2014) Shotgun microbial profiling of fossil remains. Molecular Ecology, 23:1780–1798

Fu Q et al. (2013) A revised timescale for human evolution based on ancient mitochondrial genomes Curr Biol 23:553-559

Henry AG, Hudson HF, Piperno DR (2009) Changes in starch grain morphologies from cooking. J Archaeol Sci 36:915-922

Henry AG, Piperno DR (2008) Using plant microfossils from dental calculus to recover human diet: a case study from Tell al-RaqÄ•'i, Syria. J Archaeol Sci 35:1943-1950

Human Microbiome Project Consortium (2012) Structure, function and diversity of the healthy human microbiome. Nature, 486:207–214.

Jonsson H, Ginolhac A, Schubert M, Johnson PL, Orlando L (2013) mapDamage2.0: fast approximate Bayesian estimates of ancient DNA damage parameters. Bioinformatics 29:1682-1684

Knights D, Kuczynski J, Charlson ES, Zaneveld J, Mozer MC et al. (2011) Bayesian community-wide culture-independent microbial source tracking. Nat. Methods 8:761–63

Langmead B, Salzberg SL (2012) Fast gapped-read alignment with Bowtie 2. Nat Met 9:357-359

Li H, Durbin R (2009) Fast and accurate short read alignment with Burrows-Wheeler transform. Bioinformatics 25:1754-1760

Louvel G, Der Sarkissian C, Hanghøj K, Orlando L (2016) metaBIT, an integrative and automated metagenomic pipeline for analysing microbial profiles from high-throughput sequencing shotgun data. Mol Ecol Resour. 16:1415-1427

Madella M, Alexandre A, Ball T (2005) International code for phytolith nomenclature 1.0 Ann Bot-London 96:253-260

Madella M, Lancelotti C, Garcìa-Granero JJ (2016) Millet microremains-an alternative approach to understand cultivation and use of critical crops in Prehistory. Archaeol Anthrop Sci 8:17-28

Mariotti Lippi M, Pisaneschi L, Sarti L, Lari M, Moggi-Cecchi J (2017) Insights into the Copper-Bronze Age diet in Central Italy: Plant microremains in dental calculus from Grotta dello Scoglietto (Southern Tuscany, Italy). J Archaeol Sci: Reports 15:30-39

Ondov BD, Bergman NH, Phillippy AM (2011) Interactive metagenomic visualization in a Web browser. BMC bioinformatics 12:385

Peltzer A, Jager G, Herbig A, Seitz A, Kniep C, Krause J, Nieselt K (2016) EAGER: efficient ancient genome reconstruction. Genome biol 17:60

Piperno DR (2006) Phytoliths: a Comprehensive Guide for Archaeologists and Paleoecologists. AltaMira Press, Lanham, Maryland

Schubert M et al. (2012) Improving ancient DNA read mapping against modern reference genomes. BMC genomics 13:178

Seidemann J (1966) Starke-Atlas. Grundlagen der Starke-Mikroskopie und Beschreibung der wichtigsten Starkearten vol 19. vol 11. Verlag Paul Parey, Berlin. doi:doi:10.1002/star.19670191108

Skoglund P, Northoff BH, Shunkov MV, Derevianko AP, Paabo S, Krause J, Jakobsson M (2014) Separating endogenous ancient DNA from modern day contamination in a Siberian Neandertal. P Natl Acad Sci USA 111:2229-2234

Truong DT et al. (2015) MetaPhlAn2 for enhanced metagenomic taxonomic profiling. Nat Met 12:902-903

Warinner C, Herbig A, Mann A, Fellows Yates JA, Weiß CL, Burbano HA, Orlando L, Krause J (2017) A Robust Framework for Microbial Archaeology. Annu Rev Genomics Hum Genet. 18:321-356

Warnes G et al. (2015) gplots: Various R Programming Tools for Plotting Data. R package version 2.17.0

Tables

Sample ID	Procedure	DNA concentration (ng/µl)		Average fragment length (bp)
		Agilent 2100 Bioanalyzer §	Qubit^{TM} 4 Fluorometer*	
P.O 108-7	A	7.51	3.77	77
	C	6.41	1.85	76
P.O Z. US44	A	5.31	1.87	71
	C	3.75	1.51	71
P.O 898-11	A	33.52	15.9	120
	C	23.41	11.23	97

S1 Table. Qualitative and quantitative assessment of DNA extracted from ancient dental calculus after Procedures A and C. *(* measures performed at a later period than §)*

Sample ID	Number of raw reads	Number of merged reads (%)	Mapped reads before DeDup	Mapped reads after DeDup	Cluster factor	Human DNA (%)	Number of reads on mitochondrion	5' damage (%)	3' damage (%)	Average fragment length (bp)
P.O 108-7 A	4,189,350	1,787,817 (96.61)	1,520	1,011	1.00	0.057	0	14.75	23.89	38.92
P.O Z. US44 A	12,297,890	5,570,243 (96.59)	3,817	2,470	1.001	0.046	0	23.12	22.54	40.68
P.O 898-11 A	15,930,688	7,262,574 (89.26)	6,943	5,312	1.00	0.073	0	21.35	21.75	57.29

S2 Table. Bioinformatics analysis results for human genome.

Sample ID	Number of merged non-human reads	Mapped reads on MetaPhlAn database before remove duplicates	Mapped reads on MetaPhlAn database after remove duplicates
P.O 108-7 A	1,787,817	21,671	21,029
P.O Z. US44 A	5,376,260	61,762	59,803
P.O 898-11 A	7,255,634	109,559	100,897

S3 Table. Non-human reads mapped on the MetaPhlAn2 database prior and after PCR duplicates removal

Bacterial species	Misincorporation pattern (%)		Average fragment length (bp)
	CtoT	GtoA	
SAMPLE P.O 108-7 A			
Actinomyces cardiffensis	19.15	16.61	42.01
Abiotrophia defectiva	21.11	23.34	42.37
Bacteroidetes oral taxon 274	21.31	26.81	41.55
Desulfobulbus sp oral taxon 041	22.72	25.14	42.53
Fretibacterium fastidiosum	19.14	22.71	41.18
Lautropia mirabilis	23.68	26.64	42.33
Neisseria sicca	21.26	24.15	41.84
Propionibacterium propionicum	21.45	22.51	41.71
Streptococcus sanguinis	19.81	21.76	41.79
Treponema sacranskii	18.56	19.28	40.59
SAMPLE P.O Z. US44 A			
Actinomyces cardiffensis	18.58	18.32	43.96
Abiotrophia defectiva	17.47	20.58	43.44
Bacterioidetes bacterium oral taxon 272	20.65	22.34	43.26
Bacteroidetes oral taxon 274	21.79	23.16	42.70
Desulfobulbus sp oral taxon 041	21.23	22.68	43.58
Eikenella corrodens	20.13	21.64	43.05
Fretibacterium fastidiosum	18.42	19.68	43.03
Lautropia mirabilis	20.63	22.72	42.22
Propionibacterium propionicum	19.35	21.57	42.92
Rothia aeria	21.76	22.88	42.42
Streptococcus sanguinis	17.57	19.79	42.81
Tannerella forsythia	22.11	23.97	42.65
Treponema sacranskii	18.16	20.58	41.78
SAMPLE P.O 898-11 A			
Abiotrophia defectiva	16.68	18.32	61.07
Aggregatibacter aphrophilus	18.36	20.25	60.67
Bacteroidetes oral taxon 274	16.42	18.20	62.98
Desulfobulbus sp oral taxon 041	16.03	15.30	61.67
Lautropia mirabilis	16.81	19.50	62.04
Neisseria elongata	16.97	19.70	60.61
Neisseria sicca	17.05	20.39	58.64
Propionibacterium propionicum	12.81	16.32	57.06
Rothia aeria	17.48	20.69	59.06
Streptococcus sanguinis	16.95	19.44	59.17
Tannerella forsythia	15.79	16.55	61.94

S4 Table. Deamination patterns and average fragment length for bacterial species with relative

abundance ≥ 1, assessed on the mapping reads on the relative reference genome

Sample ID	Number of raw reads	Number of merged reads (%)	Mapped reads before DeDup	Mapped reads after DeDup	Average fragment length (bp)	Mapped reads after PMDtools	Mean coverege	Contamination estimation		Hg
								Contamination (95% CI)	Pr(authentic)	
P.O 108-7 A	1,254,548	548,948 (96.53)	29,122	13,509	47.66	2,967	9.98	0.03-4.26%	99.81%	U5a1c2a1
P.O Z. US44 A	7,004,204	3,026,481 (95.64)	62,474	13,933	49.10	3,538	11.89	0.11-7.65%	99.43%	X2 + 225
P.O 898-11 A	41,276,132	16,445,256 (77.23)	292,892	93,668	58.11	20,471	109.96	9.87-23.06%	84.38%	NA

S5 Table. Bioinformatics analysis results for human mitochondrial genome.

Sample ID	Hg	Total Variants	Variants	Missing positions
P.O 108-7 A	U5a1c2a1	25	A73G, A183G, A263G, A750G, A1438G, A2706G, C7028T, A8860G, G9477A, C10544T, A11467G, G11719A, A12280G, A12308G, G12372A, T13617C, C14766T, A15218G, A15326G, C16192T, C16256T, C16270T, C16286T, C16320T, A16399G	341
P.O Z. US44 A	X2 + 225	20	A153G, A263G, A750G, A1438G, G1719A, A2706G, A4769G, T6221C, C6371T, C7028T, C8254T, A8860G, C11073T, G11719A, A13966G, T14470C, T15090C, A15326G, C16278T, T16519C	262

S6 Table. Haplogroup (Hg) assessment and mitochondrial DNA variants respect to the rCRS for two ancient samples. Last column provides the number of

unassigned positions over the complete mitogenomes